King Saud University

Saudi Pharmaceutical Journal

www.ksu.edu.sa
www.sciencedirect.com

CrossMark

ORIGINAL ARTICLE

Polymeric films as a promising carrier for bioadhesive drug delivery: Development, characterization and optimization

Pallavi Bassi, Gurpreet Kaur *

Department of Pharmaceutical Sciences & Drug Research, Punjabi University, Patiala, Punjab, India

Abstract Bioadhesive films using tamarind seed polysaccharide were prepared for the treatment of candida vaginitis using nystatin as the model drug. Films were prepared by solvent casting method. A 3^2 factorial design was employed to study the effect of independent variables (polymer and plasticizer concentration) on a range of dependent variables namely mechanical, swelling, interfacial, and bioadhesive properties through response surface methodological approach, using Design Expert® software. Formulation composition that provided the most desired and optimized results was selected using desirability approach. Nystatin was solubilized using Tween 60 and was incorporated into the selected film. Drug solubilization and dispersion were confirmed by scanning electron microscopy and differential scanning calorimetry. The optimized film released $73.92 \pm 2.54\%$ of nystatin at the end of 8 h in simulated vaginal fluid and the release data showed best fit to Korsmeyer–Peppas model with R^2 of 0.9990 and the release mechanism to be super case-II. The optimized film also showed appropriate anti candida activity through appearance of zone of inhibition during antifungal activity testing study.

1. Introduction

Polymers derived from natural sources have been reported to possess versatile applications in biomedical and pharmaceuticals. Their availability in abundance, renewability, safety and biocompatible nature has encouraged the formulation scientist to substitute them for synthetic additives. Further, the presence of large number of reactive functional groups on the polymeric backbone of polysaccharides endows them with inherent bioadhesive potential. Natural polysaccharidic bioadhesive films as dosage forms are receiving considerable attention in the pharmaceutical industry as novel, patient compliant and convenient products due to their small size and thickness (Hariharan and Bogue, 2009; Lee and Chien, 1995; Li et al., 1998; Peh and Wong, 1999). Moreover, ease of manufacturing, cost effective method of preparation and

* Corresponding author. Tel.: +91 9814724622.
E-mail address: kaurgpt@gmail.com (G. Kaur).
Peer review under responsibility of King Saud University.

ELSEVIER **Production and hosting by Elsevier**

biocompatible nature of these films have promoted their applicability for both local and systemic delivery of therapeutic agents.

Tamarind Seed Polysaccharide (TSP) is derived from seed kernels of Tamarind (*Tamarindus indica* L.), belonging to family Leguminosae, a plant indigenous to India, Bangladesh, Myanmar, Sri Lanka, Malaysia, and Thailand (El-Siddig et al., 2006). The TSP structure comprises of β (1→4)-D-glucan backbone, substituted at position 6 of the glucopyranosyl units mainly by single α-D-xylopyranosyl residues as well as by disaccharide side chains composed of β-D-galactopyranosyl-(1→2)-α-D-xylopyranosyl residues (Patel et al., 2008). TSP is a high molecular weight polysaccharide (720–880 kDa), containing glucose, xylose and galactose units, in a molecular ratio of ~3:2:1 (Freitas et al., 2005). TSP has been reported to possess mucoadhesive (Sahoo et al., 2010) and control release properties (Sumathi and Alok, 2002). It has been employed in the textile printing as a thickener (Abo-Shosha et al., 2008) and in food industry as a thickening, stabilizing and gelling agent (Nishinari et al., 2000).

Candida vaginitis is one of the most commonly occurring infection affecting the majority of women during their lifetime. The vast incidence of this infection has stimulated the need for the development of therapeutic strategies that ensure successful eradication of the infection while maintaining the safety and therapeutic efficacy of the formulation and avoid problems like first pass effect associated with systemic delivery. In this scenario, local treatment of *C. vaginitis* represents a rational choice for its management.

Nystatin is a broad spectrum polyene antibiotic, produced by *Streptomyces noursei* strains (Kaur and Kakkar, 2010). It exerts its antifungal action by binding to sterols, chiefly ergosterol of the fungal cell membrane, and the formation of barrel-like membrane-spanning channels (Coutinho and Prieto, 2003). Nystatin has both an antifungal and fungistatic activities (Recamier et al., 2010) and has been found to possess broader spectrum of activity as compared to azole antifungals (Das-Neves et al., 2008). Commercially, very few vaginal nystatin formulations are available (Mycostatin®, Nilstat®, Nadostine®). These are cream formulations that suffer from the drawbacks of being leaky and messy in nature and also require a frequent dosing regimen owing to the self-cleansing action of the vagina, namely the secretion of mucus and humid site of administration (Valenta, 2005). In order to overcome these problems researchers started working up on designing of bioadhesive vaginal formulations, which would provide an intimate contact of the formulation at target site, improve residence time and thereby provide appropriate drug release characteristics. Nystatin gels (Hombach et al., 2009) and microparticulate (Martín-Villena et al., 2013) bioadhesive formulations have been designed for vaginal delivery of nystatin, however the release of nystatin from these formulations is either too little (30% nystatin release from polyacrylic acid cysteamine conjugate gels in 7 days) (Hombach et al., 2009) or a burst release has been observed (Martín-Villena et al., 2013), indicating a need towards the development of a mucoadhesive formulation that would provide controlled drug release and vaginal residence characteristics.

Response Surface Methodology (RSM) is widely used as a tool for designing of experiments in the development and optimization of drug delivery systems (Aberturas et al., 2002; Singh et al., 2005a,b) including preformulation studies to facilitate screening of excipients and to study the effects of different formulations and/or process variables on the drug release or dissolution characteristics (Chopra et al., 2007; Hooda et al., 2012; Mennini et al., 2008).

In the present study, Tamarind seed polysaccharide (TSP) bioadhesive films were prepared employing 3^2 randomized full factorial design and optimized in terms of different properties using RSM approach. The simultaneous evaluation of the effects of formulation variables (polymer and plasticizer concentration) on mechanical, swelling and bioadhesive properties of the film was carried out to determine the optimum formulation composition using RSM approach. TSP films were tested as drug carrier systems for vaginal delivery of nystatin. In vitro drug release studies and residence time studies were carried out to ensure appropriate drug release characteristics and vaginal retention. The antifungal activity of vaginal films was also determined by observing the zone of inhibition produced in vitro.

2. Material and method

2.1. Materials

Tamarind seed polysaccharide (TSP) was received as a gift sample from Encore Natural Polymer Pvt. Ltd (Naroda, Ahmadabad, India). Propylene glycol (PG) was procured from SD Fine chemicals ltd, India. Nystatin was received as a gift sample from DSM Sinochem Pharmaceuticals, India. *Candida albicans* ATCC 10231 was purchased from Institute of Microbial Technology (IMTECH), Chandigarh, India. All reagents and chemicals were of analytical grade and used as received.

Simulated vaginal fluid (SVF) was prepared according to the previous literature report with the following composition (g L^{-1}): NaCl, 3.51; KOH, 1.40; Ca(OH)$_2$, 0.222; bovine serum albumin, 0.018; lactic acid, 2.00; acetic acid, 1.00; glycerol, 0.160; urea, 0.400 and glucose, 5.00. The mixed solution was adjusted to a pH of 4.2 (Owen and Katz, 1999).

2.2. Preparation of TSP films

TSP films were prepared by the solvent casting method (Salamat-Miller et al., 2005). Briefly TSP (1–2% w/v) was dissolved in distilled water on a magnetic stirrer (Remi equipments, Mumbai India), this was followed by the addition of plasticizer (PG; 15–20%v/v). The resulting viscous solution (50 mL) was poured into polypropylene petri plates (553.86 cm^2). The petri plates were stored at 4 °C for 24 h to remove all the entrapped air bubbles (Mura et al., 2010) and then dried in an oven (Narang Scientific Works Pvt. Ltd., New Delhi) at 50 °C for 72 h. The dried films were carefully removed and checked for any imperfections or air bubbles and stored in desiccator till use.

2.3. Experimental design for optimization

A 3^2 randomized full factorial design with replicated centre point, consisting of 13 runs (Table 1), was used for optimization of films. Response surface methodology (RSM) was used to investigate the effect of independent variables (TSP concentration; X_1 and PG (plasticizer) concentration; X_2) on a range of dependent variables. The independent variables were

Table 1 A 3^2 full factorial design with replicated centre point and the values obtained for different response variables.

Batch no.	Independent variables				Response/dependent variables						
	Coded factors		Actual factors								
	TSP[a] conc. (A)	PG[b] conc. (B)	TSP[a] conc.% w/v	PG[b] conc.% v/v	Contact angle (°) (Y1)	Spreading coefficient (Y2)	Max detachment force (mN) (Y3)	Tensile strength (N) (Y4)	%EB[c] (Y5)	WVTR[d] (g/hm^2) (Y6)	% Swelling index[e] (Y7)
T1	−1	−1	1.0	15.0	30.00	−9.27	75.00	6.41	8.91	13.80	119.21
T2	−1	0	1.0	17.5	34.00	−11.83	76.00	6.38	9.37	12.50	105.38
T3	−1	1	1.0	20.0	37.00	−13.93	72.00	6.34	9.88	12.10	102.76
T4	0	−1	1.5	15.0	21.00	−4.60	79.00	7.92	9.39	14.30	128.22
T5	0	0	1.5	17.5	24.00	−5.98	77.00	7.98	10.30	13.70	110.16
T6	0	1	1.5	20.0	27.00	−7.54	73.00	7.86	10.47	13.50	106.36
T7	1	−1	2.0	15.0	12.00	−1.51	106.00	9.77	10.71	14.90	147.86
T8	1	0	2.0	17.5	14.00	−2.06	104.00	9.82	10.78	14.50	138.65
T9	1	1	2.0	20.0	18.00	−3.39	92.00	9.95	11.56	14.10	121.73
T10	0	0	1.5	17.5	24.00	−5.98	76.00	7.89	10.51	13.70	108.26
T11	0	0	1.5	17.5	24.00	−5.98	77.00	7.11	10.33	13.50	113.13
T12	0	0	1.5	17.5	25.00	−6.22	77.00	7.82	10.24	13.70	121.49
T13	0	0	1.5	17.5	23.00	−5.21	75.00	7.89	10.41	13.60	115.30

[a] TSP: tamarind seed polysaccharide.
[b] PG: propylene glycol.
[c] EB: elongation at break.
[d] WVTR: water vapour transmission rate.
[e] Swelling index values at the end of 6 h.

evaluated at three levels. The higher and lower levels of each factor were coded as +1 and −1, respectively, and the mean value as 0 (Table 1). Contact angle (Y1), spreading coefficient (Y2), bioadhesive strength (maximum detachment force) (Y3), tensile strength (Y4), % elongation at break (%EB) (Y5), swelling index (SI) (Y6) and water vapour transmission rate (WVTR) (Y7) were used as dependent (response) variables (Table 1). Design Expert® trial version 8.0.7.1(Stat-ease Inc., Minneapolis, MN, USA) was used for performing experimental design, polynomial fitting and ANOVA results. Appropriate models were selected by comparing lacks of fit p values and R^2 values. Graphs were plotted for statistically significant models with insignificant lacks of fit at desired confidence levels. The formulations were optimized using desirability approach to select optimum combination of formulation variables (X_1 and X_2) that provide desired bioadhesive and physical, mechanical and interfacial properties of TSP films.

2.4. Mass uniformity, thickness and folding endurance

Mass uniformity of the patches was tested using an electronic digital balance (Precisa Gravimetric AG). Thickness of the films was measured at three different randomly selected positions using a digital vernier calliper and a mean value was calculated. For testing folding endurance the films were folded manually at the same place, films which got folded for ⩾300 times without breaking were said to pass this test (Patel and Poddar, 2009).

2.5. Swelling index (SI) measurement

The hydration characteristics of polymer play an important role in bioadhesion. Agar plates (2% w/v agar in simulated

vaginal fluid (SVF)) were prepared and maintained at 37 °C. The initial diameter of individual films was determined. These were then allowed to swell on the surface of the agar plates. The samples were removed at regular intervals and the increase in the diameter of the films was determined for a period of 8 h. SI was calculated from the following formula:

$$\%S\ (SI) = (D_t - D_o)/D_o * 100 \tag{1}$$

where $\%S$ is the % swelling, D_t and D_o the diameter of the swollen and original film respectively after time (Mura et al., 2010).

2.6. Determination of interfacial properties: contact angle and spreading coefficient measurement

Contact angle of SVF with surface of films was obtained by modification of a method reported by Grzegorzewski et al. (2010). A drop of SVF (200 µL) was placed gently on the top of the film surface with a micropipette from a distance of 1 cm. Images were captured using a digital camera. The angle between the tangent line of the drop and the film surface was calculated using Image J software. Spreading coefficient at the SVF and film surface was calculated using the equation:

$$S = \gamma_L(\cos\ \theta - 1) \tag{2}$$

where γ_L is the surface tension of SVF calculated using stalagmometer method (Jindal et al., 2013).

2.7. Determination of mechanical properties: tensile strength & % elongation at break (%EB) measurement

The mechanical properties of films were evaluated using texture analyser equipment equipped with a 10 Kg load cell (TA.XT plus, Stable Micro Systems, UK) (Perumal et al.,

Table 2 Lack of fit p-value and R^2 values for model selection of different response variables.

	Sequential p-value	R^2	Adjusted R^2	Predicted R^2	Lack of fit p-value	Comments
Contact angle (Y1)						
Linear	<0.0001	0.9946	0.9935	0.9913	0.8367	Suggested
2FI	0.4094	0.9950	0.9934	0.9887	0.8273	
Quadratic	0.8567	0.9952	0.9918	0.9807	0.6564	
Cubic	0.4252	0.9966	0.9919	0.9869	0.7837	Aliased
Spreading coefficient (Y2)						
Linear	<0.0001	0.9578	0.9494	0.9088	0.0450	
2FI	0.0812	0.9705	0.9606	0.8882	0.0662	
Quadratic	0.0020	0.9950	0.9914	0.9829	0.7676	Suggested
Cubic	0.5475	0.9960	0.9905	0.9873	0.8150	Aliased
Max detachment force (Y3)						
Linear	0.0021	0.7091	0.6509	0.4515	0.0003	
2FI	0.4480	0.7281	0.6375	0.1675	0.0002	
Quadratic	<0.0001	0.9905	0.9837	0.9373	0.0779	Suggested
Cubic	0.4463	0.9931	0.9835	0.4319	0.0359	Aliased
Tensile strength (Y4)						
Linear	<0.0001	0.9519	0.9423	0.9280	0.7645	Suggested
2FI	0.7013	0.9527	0.9370	0.8887	0.6977	
Quadratic	0.1520	0.9724	0.9527	0.9539	0.9849	
Cubic	0.9759	0.9727	0.9344	0.8847	0.7692	Aliased
%EB (Y5)						
Linear	<0.0001	0.9298	0.9157	0.8858	0.0601	Suggested
2FI	0.7833	0.9304	0.9072	0.8642	0.0463	
Quadratic	0.6282	0.9390	0.8955	0.5984	0.0277	
Cubic	0.7059	0.9470	0.8727	−4.2936	0.0080	Aliased
WVTR (Y6)						
Linear	<0.0001	0.9183	0.9020	0.8181	0.0190	
2FI	0.0470	0.9486	0.9314	0.8605	0.0343	
Quadratic	0.0808	0.9749	0.9570	0.7869	0.0637	Suggested
Cubic	0.0169	0.9951	0.9882	0.9784	0.7615	Aliased
Swelling index (Y7)						
Linear	0.0002	0.8242	0.7890	0.6894	0.3097	
2FI	0.4618	0.8350	0.7800	0.4729	0.2768	
Quadratic	0.0386	0.9349	0.8884	0.7713	0.7350	Suggested
Cubic	0.5502	0.9487	0.8769	0.6491	0.6801	Aliased

2008). A film strip of area 10 cm^2 was held between two clamps of texture analyser probe positioned 3 cm apart. The film strip was pulled by the upper arm (trigger load 0.05 N) at the rate of 5.0 mm/s to a distance of 100 mm before returning to the starting point. The force required to break the film and the elongation at break were measured. The calculations were performed using Texture-Pro CT V1.3 Build 14 software (Heng et al., 2003).

2.8. Determination of bioadhesive strength/maximum detachment force

The in vitro bioadhesive strength was evaluated using a texture analyser equipment (TA.XT plus, Stable Micro Systems, UK) equipped with a 100 g load cell. Fresh porcine vaginal mucosa was used as a model membrane. The mucosal membrane was obtained from slaughter house was thoroughly cleaned by removing the underlying connective tissue and washed with SVF. It was mounted securely in place on a membrane tissue holder and wetted with 0.1 mL of SVF. The mucosa was exposed to the probe through a circular disc having a cavity of diameter 1.27 cm. A sample of the prepared TSP film (1 cm^2) was attached (using double sided adhesive tape) to the base of the cylindrical probe, which was fixed to the mobile arm of the texture analyser. The cylindrical probe with the film attached to its base was lowered onto the circular disc at a speed of 0.5 mm/s and a force of 1 N for a contact time of 30 s. It was then withdrawn at a rate of 0.5 mm/s to a distance of 10 mm. The mucoadhesive performance of the samples was determined by measuring the resistance to the withdrawal of the probe (maximum detachment force) reflecting the bioadhesive characteristics of the TSP film (Eouani et al., 2001).

2.9. Determination of water vapour transmission rate (WVTR)

The WVTR (g m^{-2} h^{-1}) of TSP films was determined using a vapometer (Delfin Technologies Ltd., Kuopio, Finland). Films were mounted and sealed on the top of open specially designed beakers filled with 8.9 mL of distilled water. The system was then equilibrated for 2 h at room temperature (25 ± 2 °C, 42–46% RH) and thereafter WVTR was measured (Silva et al., 2008).

Table 3 ANOVA results for the selected models for different responses.

Response	Source	Sum of squares	DF[a]	Mean square	F value	p-Value Prob $> F$	Comments
Y1	Quadratic model	2004.0362	5	400.8072	433.1556	< 0.0001	Significant
	Lack of fit	4.8320	3	1.6107	3.9158	0.1102	Not significant
Y2	Linear model	0.7029	2	0.3514	83.2927	< 0.0001	Significant
	Lack of fit	0.0121	6	0.0020	0.2685	0.9257	Not significant
Y3	Linear model	601.6667	2	300.8333	923.8189	< 0.0001	Significant
	Lack of fit	1.2564	6	0.2094	0.4188	0.8367	Not significant
Y4	Quadratic model	151.97284	5	30.3946	277.0218	< 0.0001	Significant
	Lack of fit	0.1737	3	0.0579	0.3897	0.7676	Not Significant
Y5	Quadratic model	1576.1244	5	315.2249	146.0696	< 0.0001	Significant
	Lack of fit	11.9063	3	3.9688	4.9610	0.0779	Not significant
Y6	Linear model	18.0618	2	9.0309	98.9858	< 0.0001	Significant
	Lack of fit	0.4065	6	0.0677	0.5356	0.7645	Not significant
Y7	Linear model	5.3870	2	2.6935	66.1823	< 0.0001	Significant
	Lack of fit	0.3631	6	0.0605	5.5166	0.0601	Not significant
Y8	Quadratic model	6.5291	5	1.3058	54.4593	< 0.0001	Significant
	Lack of fit	0.1358	3	0.0453	5.6602	0.0637	Not significant
Y9	Quadratic model	2022.0026	5	404.4005	20.1006	0.0005	Significant
	Lack of fit	35.1430	3	11.7143	0.4434	0.7350	Not significant

[a] DF: degree of freedom.

2.10. Preparation of drug loaded films

The optimized TSP blank films were loaded with nystatin a 'polyene antibiotic'. It is commercially available as a mixture of three different constituents (A_1, A_2, A_3). Nystatin sample containing > 90% of constituent A_1 with a potency of 6830 units/mg as specified and supplied by the manufacturer was used in the present study.

For the preparation of drug loaded TSP films nystatin (10,000 units) was dispersed either alone (film code T14D) or in a ratio of 1:0.5 (film code T14DT$_{0.5}$) and 1:1 with Tween 60 (film code T14DT) in water. Tween 60 was used as a solubilizing agent for nystatin (Tallury et al., 2007). The nystatin dispersion was poured into TSP solution containing PG. The solutions were mixed and poured into petri-plates, which were stored at 4 °C for 24 h and subsequently dried in an oven (Narang Scientific Works Pvt. Ltd., New Delhi) at 50 °C for 72 h.

2.11. Physiochemical interaction studies

2.11.1. Differential scanning calorimetry

The physicochemical interaction among drug and other excipients incorporated in the film was characterized by carrying out the DSC (Mettler Toledo 812E, Switzerland) studies. TSP films were heated at a heating rate of 10 °C min^{-1} in the heating range of 30–400 °C under nitrogen atmosphere.

2.11.2. Scanning electron microscope characterization of films

The morphological characteristics of blank, drug loaded and drug and Tween loaded TSP films were examined using a JEOL JSM-6610 LV scanning electron microscope (SEM) (JEOL Ltd., Tokyo, Japan) operated at 15 kV. The films were coated with a layer of gold under argon atmosphere for 70 s prior to imaging at different magnifications.

2.12. Drug content uniformity

The uniformity of drug distribution in films was determined 1 cm^2 patches of T14DT films from five different locations. The patch was weighed, homogenized (Remi equipments, Mumbai, India) and dissolved in SVF with continuous stirring on a magnetic stirrer to extract the drug. The drug content was determined using the standard plot of nystatin.

## 2.13. In vitro drug release and residence time

In vitro drug release studies were carried out using simulated dynamic vaginal system (Yoo et al., 2006). This system is based upon the rate of secretion and maximum volume of mucus in the vagina. Freshly isolated porcine vaginal tissue, obtained from slaughter house, was cleaned, and cut into size of 5 × 5 cm^2. The vaginal mucosa was mounted on a glass slide inclined at an angle of 30° with the mucosal side facing upwards. The optimized drug loaded TSP film (size 1 cm^2) was mounted on the mucosal membrane. SVF was allowed to flow on the film at a rate of 5 mL h^{-1} with the help of a peristaltic pump (Electrolab, PP201V, Mumbai, India). A flask was placed under the glass slide and the perfused SVF was collected, at predetermined time intervals. The absorbance of the samples was measured at 306 nm using UV–Vis spectrophotometer and the drug release was determined by extrapolation from the calibration curve. Residence time of the films on the vaginal mucosa was also determined by using the same method (Yoo et al., 2006).

The drug release profiles were fitted into different models to determine the kinetics and mechanism of drug release. The best fit model was determined on the basis of value of coefficient of linear correlation (R^2) (Costa and Lobo, 2001).

Table 4 Values of coefficients obtained for variables X_1 and X_2 in the equations generated for different response variables.[a]

Coefficient value	Contact angle	Spreading coefficient	Maximum detachment force	Tensile strength	%EB	WVTR	Swelling index
β_0	24.08	−5.89	76.86	7.93	10.22	13.64	114.05
β_1	−9.50	4.68	13.17	1.74	0.82	0.85	13.48
β_2	3.17	−1.58	−3.83	8.33E−003	0.48	−0.55	−10.74
β_3	0.00	0.70	−2.75	0.00	0.00	0.23	−2.42
β_4	0.00	−1.02	11.98	0.00	0.00	−0.16	7.02
β_5	0.00	−0.14	−2.02	0.00	0.00	0.24	2.30

[a] The β_3, β_4, β_5 coefficient values of contact angle, tensile strength and %EB are zero since they were found to have a linear fit.
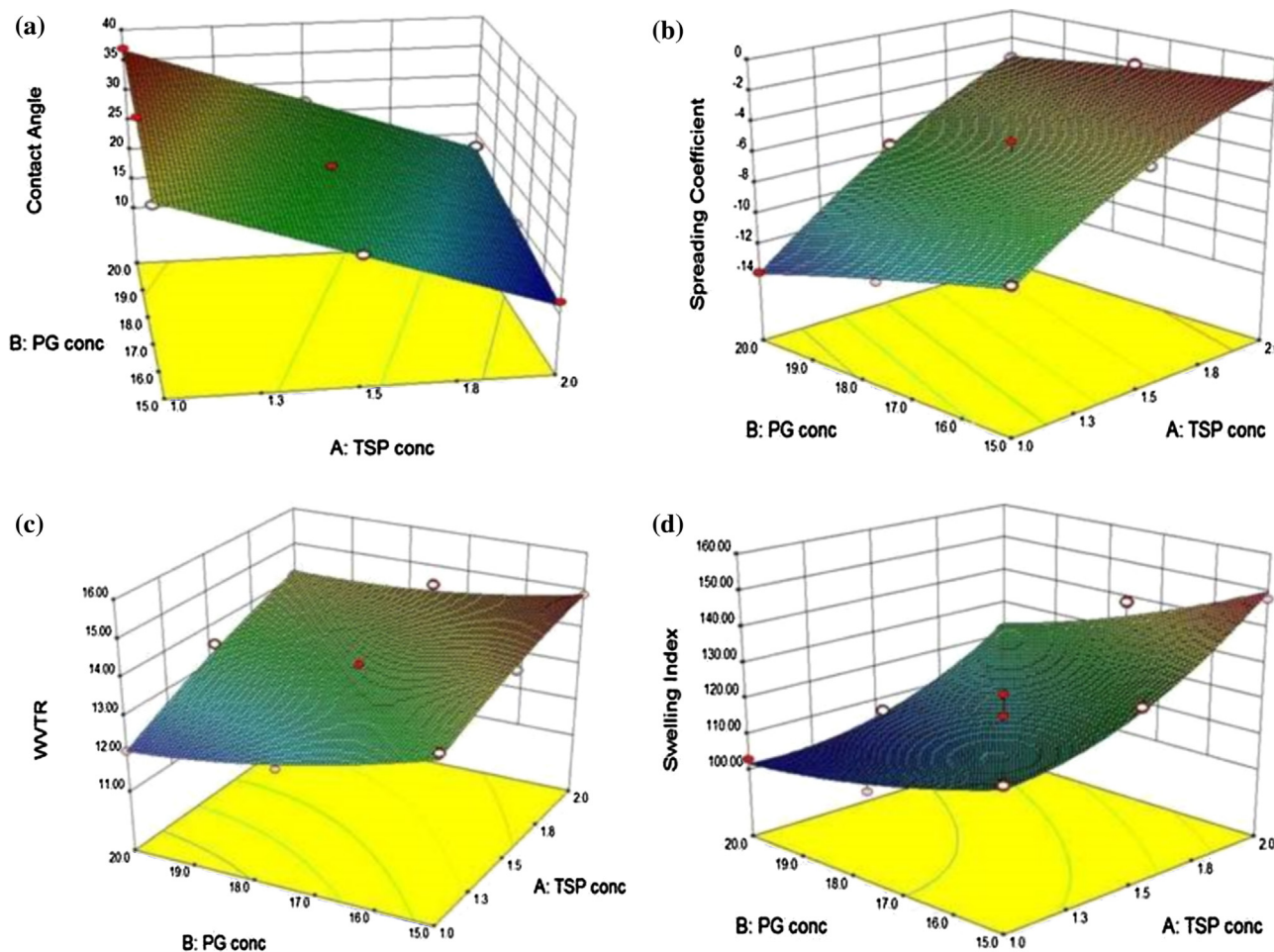
Figure 1 Response surface plots for responses namely (a) contact angle, (b) spreading coefficient, (c) WVTR, and (d) swelling index.

2.14. In vitro antifungal activity

Agar diffusion method was used for in vitro antifungal activity testing. Freeze dried samples of *C. albicans* (MTCC 227), were revived on Malt Extract Glucose Yeast Extract Peptone Broth media (MGYPB) and stored at 4 °C. The yeast was sub-cultured in Sabouraud Dextrose Agar (SDA) media, 48 h prior to antifungal activity testing. Stock inoculum suspension was prepared in sterile saline from the subculture and was adjusted to 0.5 McFarland turbidity standards to get an approximate concentration of 1×10^8 CFU mL^{-1}. The prepared SDA plates were inoculated with 0.1 mL of *C. albicans* suspension and spread uniformly with the help of a sterile spreader. Blank and drug loaded films were placed onto inoculated media plates. Tween solubilized nystatin in SVF was used as a positive control. In this case, nystatin solution equivalent to 10,000 units of nystatin, was placed in wells bored in previously inoculated SDA plates. These plates were maintained at 4 °C for 2 h before incubating them at 37 °C for 24 h. The zone of inhibition (ZOI) was determined using zone reader (Moussa et al., 2012).

2.15. Stability studies

Accelerated stability studies were carried out using a stability chamber maintained at 40 ± 0.5 °C and 75 ± 5% RH.
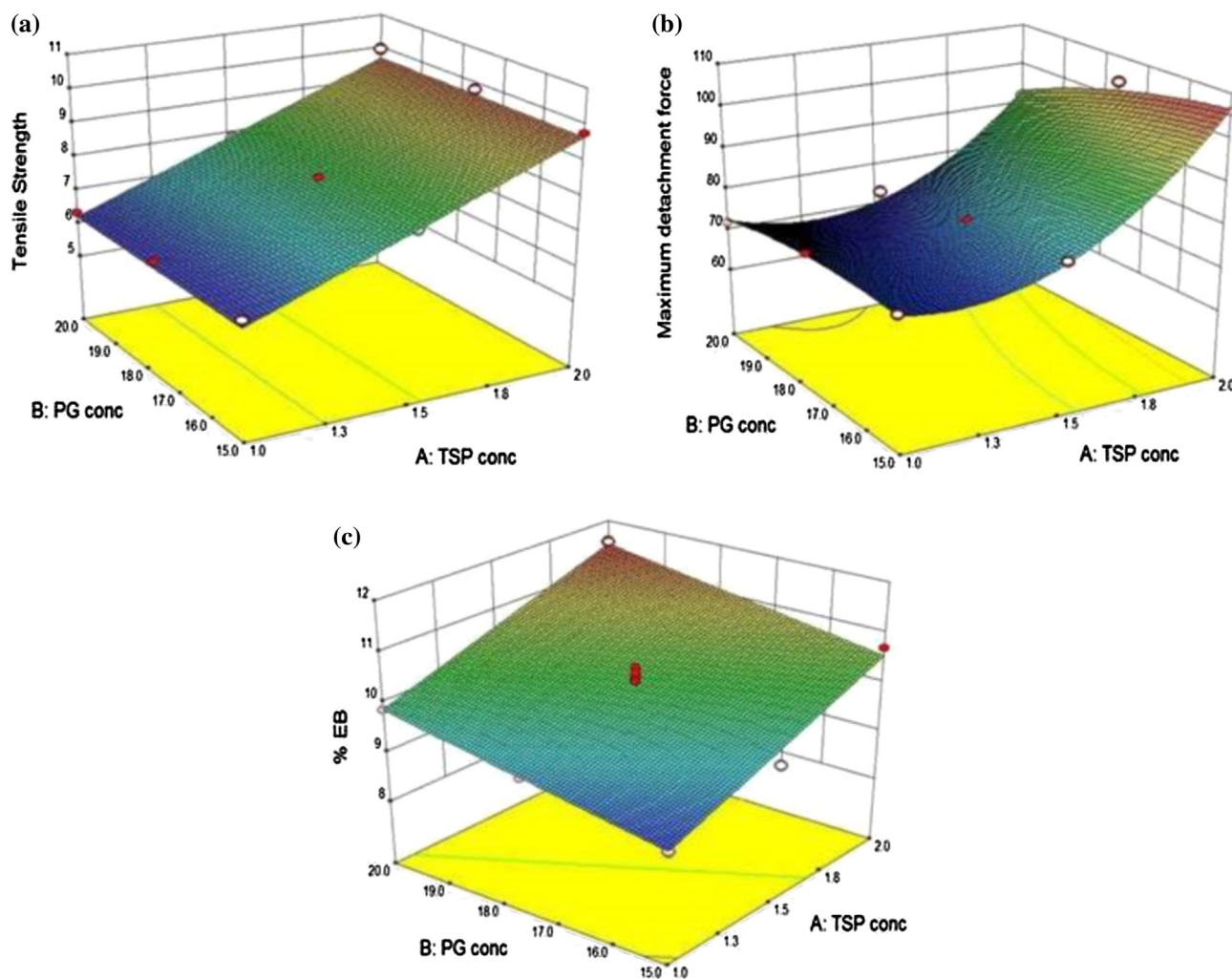
(a)

(b)

(c)

Figure 2 Response surface plots for responses namely (a) tensile strength, (b) max detachment force, and (c) %EB (% elongation at break).
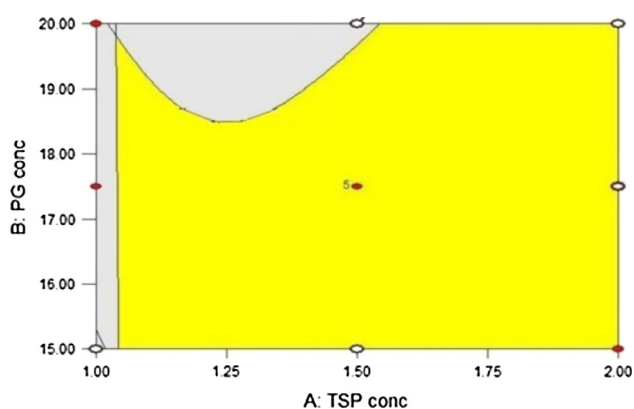

Figure 3 Overlay plot of all response variables showing the region of desirability.

T14DT films were wrapped in aluminium foil and stored in a glass container for 6 months in the stability chamber. They were evaluated for mass uniformity, thickness, folding endurance, drug content uniformity and % drug release at 0, 3 and 6 month time intervals (Palem et al., 2011; Patel and Poddar, 2009).

3. Results and discussions

3.1. Preparation of TSP films

TSP was found to display adequate film forming properties. The developed films were smooth and uniform in texture. The mass of prepared TSP films ranged from 57.18 ± 1.23 to 98.00 ± 1.28 mg, while thickness was found to be in the range of 1.52 ± 0.25 to 2.31 ± 0.09 mm. All the prepared films passed the folding endurance test.

3.2. Response Surface Methodological Optimization

A 3^2 randomized full factorial design with centre point replicated four times, consisting of 13 runs ($3 \times 3 + 4 = 13$) (Table 1) was designed and the effect of independent variables (TSP concentration; X_1 and PG (plasticizer) concentration; X_2) was studied on the response variables (Y1–Y7) using Design Expert® software trial version 8.0.7.1(Stat-ease Inc.,
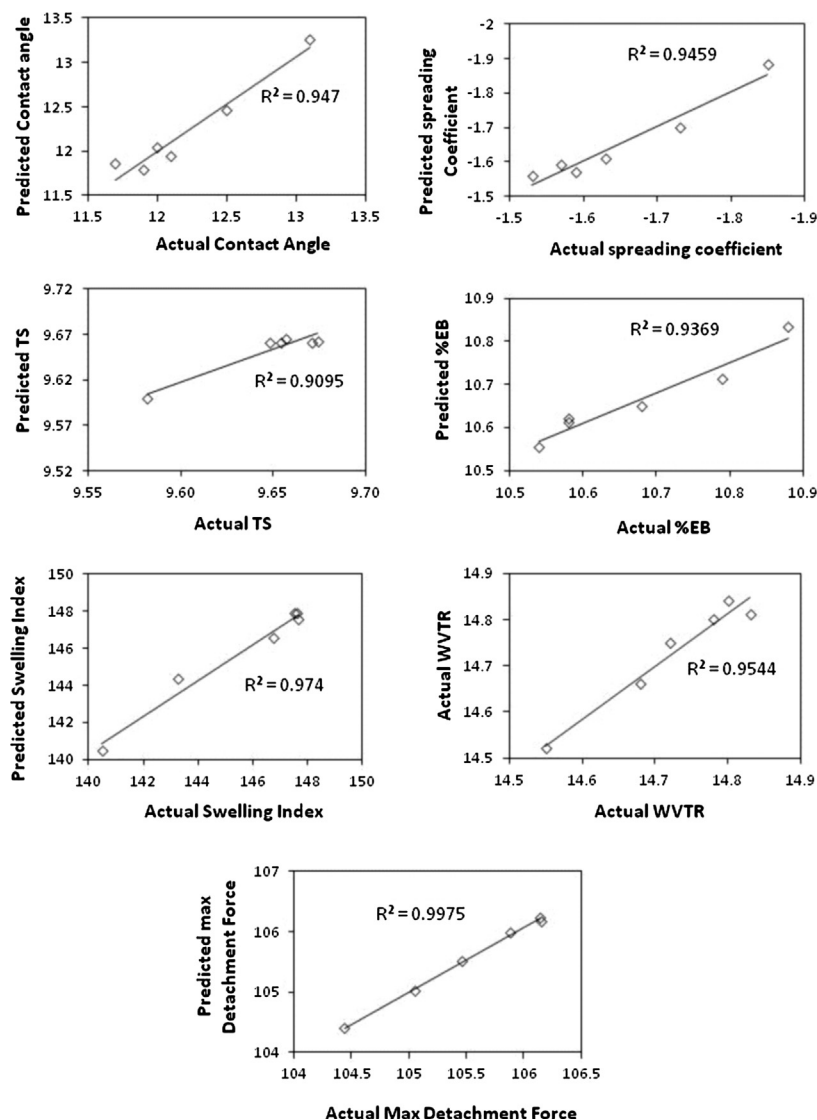
Figure 4 Linear correlation plots between actual and predicted values for different check point formulations for different responses.

Minneapolis, MN, USA). The replicate experiments were included in the design to determine whether the effect of changing factor levels is significantly larger than the effect of experimental error on responses (Santosa et al., 2005). Table 1 depicts the values of different response variables obtained for different formulations. The obtained values were fitted into different models namely linear, 2FI (2 factor interaction), Quadratic and cubic using Design Expert® software and a suitable model was selected based on lack of fit *p*-value and R^2 values. The different model fitting values are shown in Table 2. Lack of fit values depicted in the Table is indicative of how effectively the model fits the data. It measures residual error to pure error. A significant lack of fit ($p < 0.05$) is an undesirable property, because it suggests that the model does not fit the data well and hence should not be used for further predictions. Models chosen for responses Y1–Y7 had an insignificant lack of fit. The value of correlation coefficient (R^2) is also an indication of the appropriateness of the selected model. Adjusted R^2 represents the amount of variation that can be explained by the model. Predicted R^2

represents the amount of variation in predicted values explained by the model. In the present study, the predicted R^2 and the adjusted R^2 of the selected models are within 0.20 (as shown in Table 2) of each other indicating appropriateness of the selected models. A quadratic model was selected for responses Y2, Y3, Y6, Y7 and linear model was selected for responses Y1, Y4 and Y5. The statistical validity of the selected models was further established by ANOVA. The results are summarized in Table 3. From the table it can be observed that for all the responses, the model terms are significant ($p < 0.05$) and they have an insignificant lack of fit, which implies that the selected models are statistically significant and can be used for prediction of responses. The %CV and adequate precision values for responses Y1–Y7 were 2.37 and 92.413, 5.16 and 55.62, 1.80 and 35.637, 3.81 and 24.029, 1.97 and 26.794, 1.13 and 26.616, 3.79 and 15.897, respectively.

Eq. (3) is a generalized equation representing the relationship between dependent variable (Y) and independent variable (X_1 and X_2) obtained for all the responses. The coefficients of
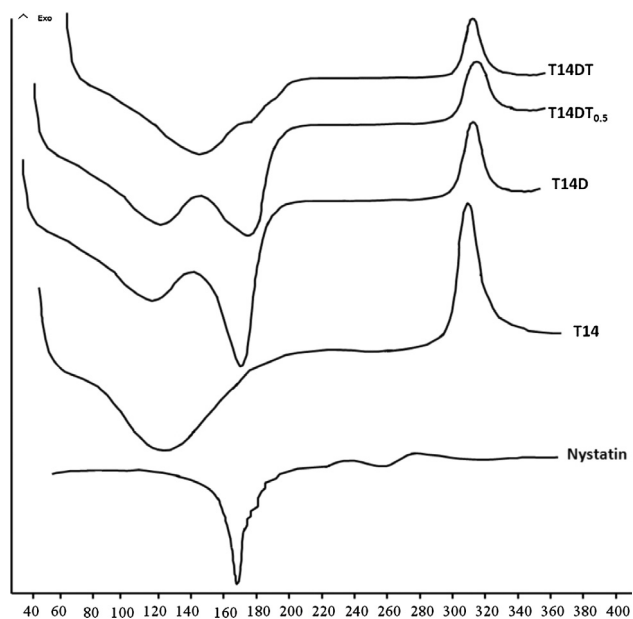
Figure 5 Physicochemical interactions between blank (T14) and drug loaded TSP films with nystatin and Tween in ratio of 1:0 (T14D), 1:0.5 (T14DT$_{0.5}$) and 1:1 (T14DT).

the variables X_1 and X_2 in Eq. (3) for different responses are compiled in Table 4.

$$Y = \beta_0 + \beta_1 X_1 + \beta_2 X_2 + \beta_3 X_1 X_2 + \beta_4 X_1^2 + \beta_5 X_2^2 \qquad (3)$$

An increase in the polymer (TSP) concentration has a positive impact on the spreading coefficient, maximum force required for detachment, tensile strength, %EB, WVTR and

swelling index. However, a decrease in the value of contact angle was observed with an increase in TSP. The swelling index, spreading coefficient, WVTR and maximum force required for detachment properties of a polymer are a function of the number of hydrophilic groups available for interaction with the mucus. An increase in the concentration of polymer increases the number of available groups, thereby increasing the magnitude of these properties. Further, an increase in polymer concentration also improves the contact with mucus which leads to a decrease in contact angle values (Patel et al., 2011; Salamat-Miller et al., 2005). An increase in plasticiser concentration increases the hydrophobic character of the films (Orliac et al., 2003) resulting in a decreased affinity between film surface and mucus membrane and therefore a trend opposite to that of increasing polymer concentration was observed (Andrews et al., 2009; Edsman and Hagerstrom, 2005). These interactive effects of the formulation variable on the response variable can be easily visualized by 3D plots shown in Figs. 1 and 2. For swelling index studies films containing 1% TSP eroded at the end of 6 h while others remained intact till the end of the study.

After establishment and analysis of appropriate models for individual responses, the simultaneous optimization of multiple responses was carried out using Design-Expert® software to find a combination of factor levels that simultaneously satisfy the requirements placed on each of the responses and factors. This process identifies those areas in design region where the system is likely to give desirable responses (Espinoza-Escalante et al., 2007; Vera-Candioti et al., 2006). This was done graphically by overlaying critical response contours on a contour plot and identifying area of feasible response values in the factor space (yellow/lighter area in Fig. 3) as well as numerically by using desirability approach. For calculating desirability function, a desired goal (maximum, minimum,
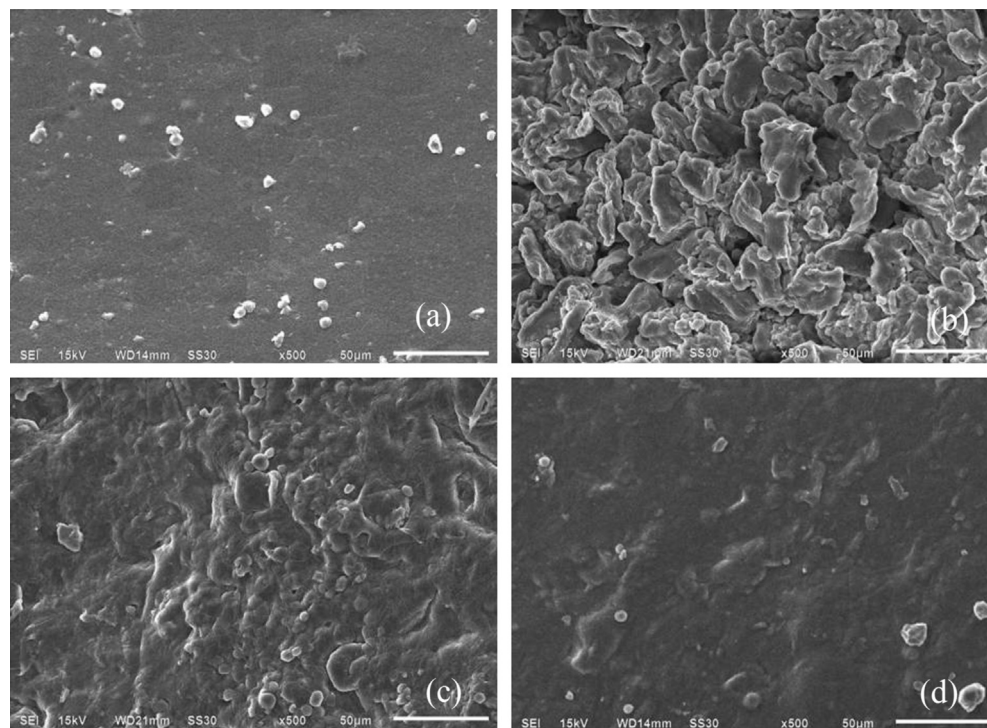

Figure 6 Surface morphology of blank (a), drug loaded TSP films with nystatin and Tween in ratio of 1:0 (b), 1:0.5 (c), and 1:1 (d).

target or within range value) was chosen for each independent and response variable. The goals are then combined into a simultaneous objective function, desirability, 'D' which is a geometric mean of all transformed responses, calculated according to the following formula:

$$D = \left(d_1^{r_1} + d_1^{r_2} \ldots \ldots d_1^{r_1}\right)^{\frac{1}{\Sigma r_1}} = \left(\prod_{i=1}^{n} d_i^{r_1}\right)^{\frac{1}{\Sigma r_1}} \tag{4}$$

where (d_i) is the desirable range for each response, (r_i) is the importance attached to various responses and (n) is the number of responses. Desirability is an objective function that ranges from zero (least desirable) to one (most desirable). Desirability is only a mathematical method to find the optimum, therefore, the goal of this optimization was to find a point that maximizes the desirability function, and meet goals set for all responses, and not just to obtain a high value. In the present research, after goal setting of all the responses, the maximum value of desirability was found to be 0.400. The optimization step gave 6 check point formulations in the desirable range and predicted 2% TSP and 15.3% v/v PG as the most desirable formulation. The other desirable formulations compositions in decreasing order of desirability were 2% TSP: 15.3% v/v PG > 2% TSP: 15.5% v/v PG > 2% TSP: 15.8% v/v PG > 2% TSP: 16.5% v/v PG > 2% TSP: 15.2% v/v PG.

3.3. Experimental verification

The check point formulations and their predicted responses were verified experimentally. All the formulations were prepared and the values of response variables were found out experimentally. The model predicted values were then compared with actual values obtained after experimentation and the percentage error in prognosis was calculated. The error was found to vary between −1.8352% and 1.8017%. Linear correlation plot between the actual and the predicted response variables is shown in Fig. 4. The plot demonstrated a high values of R^2 (ranging 0.9095–0.9975) indicating excellent goodness of fit ($p < 0.001$). Thus, the low magnitude of percentage error, as well as the significant values of R^2 in the present investigation, proved the high predictability of the RSM. Further, a two tailed t-test was also applied to the predicted and actual values of all the responses and it was found that the difference in the two values was statistically insignificant, which further confirms the predictability of the designed model. Based on the above findings formulation containing 2% TSP and 15.3% v/v PG (film code T14) was selected for drug loading and further studies. The film was loaded with nystatin (film code T14D) alone or in combination with Tween 60. Tween 60 was incorporated into the films to aid solubilization of nystatin in the ratio of 1:0.5 (film code T14DT$_{0.5}$) and 1:1 (film code T14DT) nystatin to Tween ratio.

3.4. Physiochemical interaction studies

Fig. 5 shows the DSC profiles of T14, T14D, T14DT$_{0.5}$, T14DT and nystatin. The thermal behaviour of the films can provide an insight into the drug–polymer compatibility, miscibility and any alteration in the chemical structure of either polymer or drug. DSC of pure nystatin revealed an endotherm which peaks

at 173 °C with corresponding ΔH value of 238 J g^{-1}. DSC of T14 film shows an initial endotherm followed by an exotherm with peaks at 120 °C and 309 °C, respectively. When nystatin was incorporated into the film (T14D) an additional sharp peak corresponding to the melting peak of nystatin is observed at 172 °C ($\Delta H = 155$ J g^{-1}) indicating the presence of crystalline un-solubilized drug. This peak however, reduced in intensity and enthalpy ($\Delta H = 64$ J g^{-1}) with the addition of small quantity of Tween (T14DT$_{0.5}$) and completely disappeared when the quantity of Tween was increased (T14DT). The decline in enthalpy and intensity indicates only partial solubilization of nystatin in the film indicating that 1:0.5 ratio of drug to Tween is not sufficient to cause complete solubilization of the incorporated drug. The absence of nystatin melting peak in T14DT indicates transformation of crystalline drug into amorphous state as a consequence of solubilization effect of Tween. Tween 60 was able to cause micellar solubilization of nystatin. This conclusion can be further supported by the fact that the concentration of Tween 60 used in T14DT was greater than its critical micellar concentration value (30 µg mL^{-1}) thus, ensuring formation of micelles and nystatin solubilization (Tallury et al., 2007).

SEM analysis of the film (Fig. 6) also confirmed the above findings. Blank TSP films (T14) (Fig. 6a) showed smooth texture indicating uniformity of polymer matrix. The un-solubilized drug particles were clearly evident in T14D films (Fig. 6b). Addition of Tween in T14DT$_{0.5}$ (Fig. 6c) partially solubilized nystatin and also created some smoothness in the film texture, while a completely smooth texture with no visible drug particles was observed for T14DT films (Fig. 6d). Based on the above findings that T14DT films were used for drug release studies.

3.5. Drug content uniformity, in vitro drug release and residence time

The drug content of T14DT was found to be $98.23 \pm 0.67\%$ suggesting that the film casting process led to the development of films with uniform drug dispersion.

The in vitro drug release studies were carried out on T14DT films loaded with nystatin solubilized with Tween. Samples were collected at fixed intervals, and the amount of nystatin released from the formulation with respect to time was calculated. The bioadhesive film formulation was releasing $73.92 \pm 2.54\%$ of nystatin (Fig. 7) at the end of 8 h. Release data from the films was subjected to model fitting equations namely, zero order, first order, Higuchi, Weibull and Korsmeyer–Peppas model in order to determine the rate of
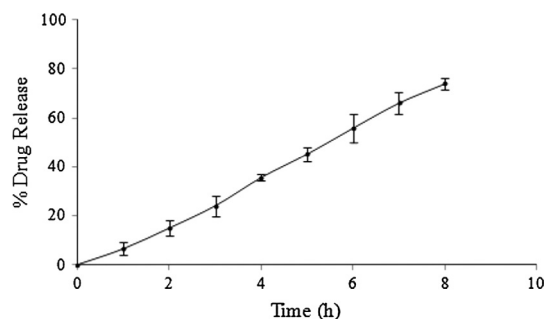

Figure 7 Nystatin release profile for TSP films.

Table 5 Stabiliy studies for T14DT films.

Parameter	0 Month	3 Months	6 Months
Mass (mg)	103.4 ± 1.04	103.4 ± 0.70	102.73 ± 0.56
Thickness (mm)	2.04 ± 0.03	2.03 ± 0.02	2.03 ± 0.02
Folding endurance	>300	>300	>300
% Drug content	98.23 ± 0.67	98.29 ± 0.64	98.21 ± 0.68
% Drug release	73.92 ± 2.54	73.49 ± 0.99	73.24 ± 0.74

drug release. The release data showed best fit to Korsmeyer–Peppas model with R^2 of 0.9996. The value of release exponent n was calculated to be 1.19, suggesting the release mechanism to be super case-II.

Residence time of the formulation was found to be about 510 ± 5 min.

3.6. In vitro antifungal activity

Tamarind has been shown to possess antifungal activity against *C. albicans*. This activity has been ascribed to the presence of some essential oils or secondary metabolites. However, several other studies have completely ruled out any such activity (Debnath et al., 2011; Doughari, 2006; Escalona-Arranz et al., 2010). In order to explore this fact and to see whether TSP can exert any synergistic anti candida activity along with the nystatin incorporated in the film, blank TSP films were subjected to antifungal activity testing. Films with different TSP concentrations (1%, 1.5%, 2% w/v TSP) namely T1, T4 and T7 were placed on the inoculated SDA plates and were observed for appearance of ZOI at the end of the study. No ZOI was observed for the blank TSP films. Absence of ZOI in blank TSP films may be correlated with loss of essential oil/secondary metabolites (which are proposed to have antifungal activity in the literature) during the extraction process of TSP. Thus, synergistic antifungal effect from the polymer can be ruled out in drug loaded TSP films in the present study.

For antifungal activity of drug loaded films, T14DT films were placed on the inoculated SDA plates and were observed for appearance of ZOI against T14 films and nystatin solution acting as the negative and positive control groups respectively. A ZOI of 1.1 ± 0.2 cm was observed for T14DT films. ZOI for nystatin solution was 1.5 ± 0.1 cm, while no ZOI was observed for T14 films. These results indicate antifungal characteristics of the prepared film.

3.7. Stability studies

For assessment of film stability three time points (0, 3, 6 months) were used. T14DT was assessed for mass uniformity, thickness, folding endurance, drug content and % drug release at each time point. The results are shown in Table 5. No significant difference ($p < 0.05$) was observed in these properties indicating that the films remained stable throughout the study period.

4. Conclusion

Bioadhesive vaginal films containing tamarind seed polysaccharide were successfully prepared and characterized for their bioadhesive, mechanical, swelling and interfacial properties and optimized using response surface methodology. The results of RSM optimization indicated that the formulation containing 2% TSP and 15.3% v/v PG possessed most desirable properties. The optimized formulation was loaded with micellar solubilized nystatin. These were able to release $73.92 \pm 2.54\%$ of nystatin and also exhibited appropriate residence time in vitro. The drug release followed Korsmeyer–Peppas kinetics with R^2 of 0.9990. The optimized film also showed appropriate anti candida activity through appearance of zone of inhibition during antifungal activity testing study. Thus, the developed TSP films can be proposed as a befitting candidate for vaginal delivery of drugs.

References

Aberturas, M.R., Molpeceres, J., Guzman, M., Garcia, F., 2002. Development of a new cyclosporine formulation based on poly(-caprolactone) microspheres. J. Microencap. 19, 61–72.

Abo-Shosha, M.H., Ibrahim, N.A., Allam, E., El-Zairy, E., 2008. Preparation and characterization of polyacrylic acid/karaya gum and polyacrylic acid/tamarind seed gum adducts and utilization in textile printing. Carbohydr. Polym. 74, 241–249.

Andrews, G.P., Laverty, T.P., Jones, D.S., 2009. Mucoadhesive polymeric platforms for controlled drug delivery. Eur. J. Pharm. Biopharm. 71, 505–518.

Chopra, S., Patil, G.V., Motwani, S.K., 2007. Release modulating hydrophilic matrix systems of losartan potassium: optimization of formulation using statistical experimental design. Eur. J. Pharm. Biophar. 66, 73–82.

Costa, P., Lobo, J.M.S., 2001. Modeling and comparison of dissolution profiles. Eur. J. Pharm. Sci. 13, 123–133.

Coutinho, A., Prieto, M., 2003. Cooperative partition model of nystatin interaction with phospholipid vesicles. Biophys. J. 84, 3061–3078.

Das-Neves, J., Pinto, E., Teixeira, B., Dias, G., Rocha, P., Cunha, T., Santos, B., Amaral, M.H., Bahia, M.F., 2008. Local treatment of vulvovaginal candidosis. Drugs 68, 1787–1802.

Debnath, S., Rahman, S.M.H., Deshmukh, G., Duganath, N., Pranitha, C., Chiranjeevi, A., 2011. Antimicrobial screening of various fruit seed extracts. Pharmacogn. J. 3, 83–86.

Doughari, J.H., 2006. Antimicrobial activity of Tamarindus indica Linn. Trop. J. Pharm. Res. 5, 597–603.

Edsman, K., Hagerstrom, H., 2005. Pharmaceutical applications of mucoadhesion for the non oral routes. J. Pharm. Pharmacol. 57, 3–22.

El-Siddig, K.E., Gunasena, H.P.M., Prasad, B.A., Pushpakumara, D.K.N.G., Ramana, K.V.R., Vijayanand, P., Williams, J.T., 2006. Tamarind, Tamarindus indica. Southampton Centre for Underutilised Crops, Southampton.

Eouani, C., Piccerelle, P., Prinderre, P., Bourret, E., Joachim, J., 2001. In-vitro comparative study of buccal mucoadhesive performance of different polymeric films. Euro. J. Pharm. Biopharm. 52, 45–55.

Escalona-Arranz, J.C., Péres-Roses, R., Urdaneta-Laffita, I., Camacho-Pozo, M.I., Rodríguez-Amado, J., Licea-Jiménez, I., 2010. Antimicrobial activity of extracts from Tamarindus indica L. leaves. Pharmacogn. Mag. 6, 242–247.

Espinoza-Escalante, F.M., Pelayo-Ortiz, C., Gutierrez-Pulido, H., Gonzalez-lvarez, V., Alcaraz-Gonzalez, V., Bories, A., 2007. Multiple response optimization analysis for pretreatments of Tequila's stillages for VFAs and hydrogen production. Bioresour. Technol. 99, 5822–5829.

Freitas, R.A., Martin, S., Santos, G.L., Valenga, F., Buckeridge, M.S., Reicher, F., Sierakowski, M.R., 2005. Physico-chemical properties of seed xyloglucans from different sources. Carbohydr. Polym. 60, 507–514.

Grzegorzewski, F., Sascha, R., Kroh, L.W., Geyer, M., Schluter, O., 2010. Surface morphology and chemical composition of lamb's lettuce (Valerianella locusta) after exposure to a low-pressure oxygen plasma. Food Chem. 122, 1145–1152.

Hariharan, M., Bogue, A., 2009. Orally dissolving film strips: the final evolution of orally dissolving dosage forms. Drug Deliv. Technol. 9, 24–29.

Heng, P.W.S., Chan, L.W., Ong, K.T., 2003. Influence of storage conditions and type of plasticisers on ethylcellulose and acrylate films formed from aqueous dispersions. J. Pharm. Pharm. Sci. 6, 334–344.

Hombach, J., Palmberger, T.F., Bernkop-Schnurch, A., 2009. Development and In vitro evaluation of a mucoadhesive vaginal delivery system for nystatin. J. Pharm. Sci. 98, 555–564.

Hooda, A., Nanda, A., Jain, M., Kumar, V., Rathee, P., 2012. Optimization and evaluation of gastroretentive ranitidine HCl microspheres by using design expert software. Int. J. Bio. Macromol. 51, 691–700.

Jindal, M., Kumar, V., Rana, V., Tiwary, A.K., 2013. Physico-chemical, mechanical and electrical performance of bael fruit gum–chitosan IPN films. Food Hydrocolloid. 30, 192–199.

Kaur, I.P., Kakkar, S., 2010. Topical delivery of antifungal agents. Expert Opin. Drug Deliv. 7, 1303–1327.

Lee, Y., Chien, Y., 1995. Oral mucosa controlled delivery of LHRH by bilayer mucoadhesive polymer systems. J. Control. Release 37, 251–261.

Li, C., Bhatt, P.P., Johnston, T.P., 1998. Evaluation of a mucoadhesive buccal patch for delivery of peptides: in vitro screening of bioadhesion. Drug Dev. Ind. Pharm. 24, 919–926.

Martín-Villena, M.J., Fernández-Campos, F., Calpena-Campmany, A.C., Bozal-de Febrer, N., Ruiz-Martínez, M.A., Clares-Naveros, B., 2013. Novel microparticulate systems for the vaginal delivery of nystatin: development and characterization. Carbohydr. Polym. 94, 1–11.

Mennini, N., Furlanetto, S., Maestrelli, F., Pinzauti, S., Mura, P., 2008. Response surface methodology in the optimization of chitosan–Ca pectinate bead formulations. Eur. J. Pharm. Sci. 35, 318–325.

Moussa, A., Noureddine, D., Saad, A., Abdelmelek, M., Abdelkader, B., 2012. Antifungal activity of four honeys of different types from Algeria against pathogenic yeast: Candida albicans and Rhodotorula sp. Asian Pac. J. Trop. Biomed. 2, 554–557.

Mura, P., Corti, G., Cirri, M., Maestrelli, F., Mennini, N., Bragagni, M., 2010. Development of mucoadhesive films for buccal administration of flufenamic acid: effect of cyclodextrin complexation. J. Pharm. Sci. 99, 3019–3029.

Nishinari, K., Yamatoya, K., Shirakawa, M., 2000. Xyloglucan. In: Phillips, G.O., Williams, P.A. (Eds.), Handbook of Hydrocolloids. Woodhead Publishing Ltd., Cambridge, pp. 247–267.

Orliac, O., Rouilly, A., Silvestre, F., Rigal, L., 2003. Effects of various plasticizers on the mechanical properties, water resistance and aging of thermo-moulded films made from sunflower proteins. Ind. Crop. Prod. 18, 91–100.

Owen, D.H., Katz, D.F., 1999. A vaginal fluid stimulant. Contraception 59, 91–95.

Palem, C.R., Gannu, R., Doodipala, N., Yamsani, V.V., 2011. Transmucosal delivery of domperidone from bilayered buccal patches: in vitro, ex vivo and in vivo characterization. Arch. Pharm. Res. 34, 1701–1710.

Patel, R.S., Poddar, S.S., 2009. Development and characterization of mucoadhesive buccal patches of salbutamol sulphate. Curr. Drug Deliv. 60, 140–144.

Patel, T.R., Morris, G.A., Ebringerova, A., Vodenicarova, M., Velabny, V., Ortega, A., Torre, J.G., Harding, S.E., 2008. Global conformation analysis of irradiated xyloglucans. Carbohydr. Polym. 74, 845–851.

Patel, V.F., Liu, F., Brown, M.B., 2011. Advances in oral transmucosal drug delivery. J. Control. Release 153, 106–116.

Peh, K., Wong, C., 1999. Polymeric films as vehicle for buccal delivery: swelling, mechanical, and bioadhesive properties. J. Pharm. Pharm. Sci. 2, 53–61.

Perumal, V.A., Lutchman, D., Mackraj, I., Govender, T., 2008. Formulation of monolayered films with drug and polymers of opposing solubilities. Int. J. Pharm. 358, 184–191.

Recamier, K.S., Hernandez-Gomez, A., Gonzalez-Damian, J., Ortega-Blake, I., 2010. Effect of membrane structure on the action of polyenes: I. Nystatin action in cholesterol and ergosterol-containing membranes. J. Membr. Biol. 237, 31–40.

Sahoo, S., Sahoo, R., Nayak, P.L., 2010. Tamarind seed polysacharide: a versatile biopolymer for mucoadhesive applications. J. Pharm. Biomed. Sci 8, 1–12.

Salamat-Miller, N., Chittchang, M., Johnston, T.P., 2005. The use of mucoadhesive polymers in buccal drug delivery. Adv. Drug Deliv. Rev. 57, 1666–1691.

Santosa, K.S.C.R., Silvaa, H.S.R.C., Ferreiraa, E.I., Bruns, R.E., 2005. 3^2 Factorial design and response surface analysis optimization of N-carboxybutylchitosan synthesis. Carbohydr. Polym. 59, 37–42.

Silva, C.L., Pereira, J.C., Ramalho, A., Pais, A., Sousa, J., 2008. Films based on chitosan polyelectrolyte complexes for skin drug delivery: development and characterization. J. Membr. Sci. 320, 268–279.

Singh, B., Dahiya, M., Saharan, V., Ahuja, N., 2005a. Optimizing drug delivery systems using systematic "design of experiments"—part II: retrospect and prospects. Critical Rev. Ther. Drug Carr. Syst. 22, 215–294.

Singh, B., Mehta, G., Kumar, R., Bhatia, A., Ahuja, N., Katare, O.P., 2005b. Design, development and optimization of nimesulide-loaded liposomal systems for topical application. Curr. Drug Deliv. 2, 143–153.

Sumathi, S., Alok, R., 2002. Release behavior of drugs from tamarind seed polysaccharide tablets. J. Pharm. Pharm. Sci. 5, 12–18.

Tallury, P., Randall, M.K., Thaw, K.L., Preisser, J.S., Kalachandra, S., 2007. Effects of solubilizing surfactants and loading of antiviral antimicrobial and antifungal drugs on their release rates from ethylene vinyl acetate copolymer. Dent. Mater. 23, 977–982.

Valenta, C., 2005. The use of mucoadhesive polymers in vaginal delivery. Adv. Drug Deliv. Rev. 57, 1692–1712.

Vera-Candioti, L., Robles, J.C., Mantovani, V.E., Goicoechea, H.C., 2006. Multiple response optimization applied to the development of a capillary electrophoretic method for pharmaceutical analysis. Talanta 69, 140–147.

Yoo, J.W., Dharmala, K., Lee, C.H., 2006. The physicodynamic properties of mucoadhesive polymeric films developed as female controlled drug delivery system. Int. J. Pharm. 309, 139–145.